TISSUE ENGINEERING: Part A
Volume 23, Numbers 1 and 2, 2017
Mary Ann Liebert, Inc.
DOI: 10.1089/ten.tea.2016.0126

termis
Tissue Engineering
& Regenerative Medicine
International Society

ORIGINAL ARTICLE

Dynamic Autologous Reendothelialization of Small-Caliber Arterial Extracellular Matrix: A Preclinical Large Animal Study

Nitsan Dahan, PhD,[1,*] Udi Sarig, PhD,[1,2,*] Tomer Bronshtein, PhD,[1] Limor Baruch, PhD,[1] Tony Karram, MD, PhD,[3] Aaron Hoffman, MD, PhD,[3] and Marcelle Machluf, PhD[1,2]

Effective cellularization is a key approach to prevent small-caliber (<4 mm) tissue-engineered vascular graft (TEVG) failure and maintain patency and contractility following implantation. To achieve this goal, however, improved biomimicking designs and/or relatively long production times (typically several months) are required. We previously reported on porcine carotid artery decellularization yielding biomechanically stable and cell supportive small-caliber (3–4 mm diameter, 5 cm long) arterial extracellular matrix (scaECM) vascular grafts. In this study, we aimed to study the scaECM graft patency *in vivo* and possibly improve that patency by graft pre-endothelialization with the recipient porcine autologous cells using our previously reported custom-designed dynamic perfusion bioreactor system. Decellularized scaECM vascular grafts were histologically characterized, their immunoreactivity studied *in vitro*, and their biocompatibility profile evaluated as a xenograft subcutaneous implantation in a mouse model. To study the scaECM cell support and remodeling ability, pig autologous endothelial and smooth muscle cells (SMCs) were seeded and dynamically cultivated within the scaECM lumen and externa/media, respectively. Finally, endothelialized-only scaECMs—hypothesized as a prerequisite for maintaining graft patency and controlling intimal hyperplasia—were transplanted as an interposition carotid artery graft in a porcine model. Graft patency was evaluated through angiography online and endpoint pathological assessment for up to 6 weeks. Our results demonstrate the scaECM-TEVG biocompatibility preserving a structurally and mechanically stable vascular wall not just following decellularization and recellularization but also after implantation. Using our dynamic perfusion bioreactor, we successfully demonstrated the ability of this TEVG to support *in vitro* recellularization and remodeling by primary autologous endothelial and SMCs, which were seeded on the lumen and the externa/media layers, respectively. Following transplantation, dynamically endothelialized scaECM-TEVGs remained patent for 6 weeks in a pig carotid interposition bypass model. When compared with nonrevitalized control grafts, reendothelialized grafts provided excellent antithrombogenic activity, inhibited intimal hyperplasia formation, and encouraged media wall infiltration and reorganization with recruited host SMCs. We thus demonstrate that readily available decellularized scaECM can be promptly revitalized with autologous cells in a 3-week period before implantation, indicating applicability as a future platform for vascular reconstructive procedures.

Keywords: bioreactors, blood vessel, endothelial cells, extracellular matrix, smooth muscle

Introduction

Autologous blood vessels for arterial bypassing remain the gold standard treatment for small-caliber (<4 mm) arterial diseases despite their limited sourceability and related morbidity at the donor site,[1] providing a strong impetus for R&D on tissue-engineered vascular grafts (TEVGs). Several TEVG strategies have been therefore suggested in recent years, utilizing either cell sheet-based self-assembly techniques[2] or biodegradable

[1]Faculty of Biotechnology and Food Engineering, Technion–Israel Institute of Technology, Haifa, Israel.
[2]School of Materials Science and Engineering, Nanyang Technological University (NTU), Singapore, Singapore.
[3]Department of Vascular Surgery and Transplantation, Rambam Health Care Campus, Technion–Israel Institute of Technology, Haifa, Israel.
*Both these authors contributed equally to this work.

synthetic/natural scaffold-guided tissue engineering approaches[1] with the aim of generating viable substitutes for autologous small-caliber grafting. Both approaches displayed some promising results *in vitro*, *in vivo*, and even in several case studies and ongoing clinical trials; however, neither has of yet been translated into wide clinical applications.[1,3,4] For instance, despite the great promise of cell sheet-based self-assembly techniques, their production process is labor-intensive, requires costly bioreactor work, and involves long *in vitro* manipulation periods (typically >12 weeks).[1,3]

Among the scaffold-based approaches, a distinction should be made between traditional *in vitro* tissue engineering—which is usually bioreactor based with all associated time, labor, and cost implications—and more trendy *in situ*/*in vivo* tissue engineering.[5] The latter has been suggested to minimize *in vitro* manipulation by using the body as a bioreactor and exploiting the host cells' potential to regenerate an implanted biodegradable scaffold (acellular or preseeded). However, the *in situ*/*in vivo* approach may suffer from issues of morbidity at the preimplantation site (if different than the graft target) and may be limited by our understanding of complex biological mechanisms involved in tissue regeneration.

Natural decellularized extracellular matrix (ECM)-based TEVGs were found to ideally preserve the vascular wall structural complexity, the biomechanical properties, and the required bioactivity that may enable proper grafting and improve tissue regeneration and function.[1,3,4] These scaffolds may represent a compromise between traditional *in vitro* and more advanced *in situ* tissue engineering, in that they can not only be preconditioned in a bioreactor *in vitro* but also be intrinsically bioactive *in vivo* in recruiting an adequate host cell regenerative response following implantation.[6] Major issues of concern, though, relate to their ability to maintain graft patency, flexibility, and contractility following implantation. In particular, thrombosis, or blood clotting, continues to be the main cause of early graft failure, while intimal hyperplasia—unregulated cell proliferation resulting in vessel occlusion—is the major cause of later graft failure.[7,8]

Precellularization of the vascular graft is, therefore, suggested as a promising regenerative medicine approach to improve graft patency and function.[1,9] Two major cell types reside within the natural blood vessel: endothelial cells (ECs) on the luminal side and smooth muscle cells (SMCs) in the vascular wall. Endothelialization—the process of graft lumen coating with a semipermeable and thromboresistant EC barrier—masks the ECM collagen thromboactive moieties and is thereby hypothesized to inhibit graft failure by preventing coagulation, increasing patency rates, and improving overall graft function. ECs affect key physiological and pathological parameters, including blood flow and vessel tone,[10] platelet activation, adhesion and aggregation,[11] leukocyte adhesion,[12] and SMC migration and proliferation.[13] EC control of SMCs is of particular importance given the SMC physiological role in contractility and their pathological involvement in late graft failure through intimal hyperplasia.[14] To avoid such long-term complications, therefore, endothelialization should ideally occur either before or quickly following implantation.

We previously reported the *in vitro* revitalization of decellularized porcine carotid (small-caliber) arterial extracellular matrix (scaECM) when dynamically cultivated using a perfusion bioreactor designed in our laboratory.[15] In this study, we further explored the clinical potential of such ECM-based revitalized arterial grafts to achieve graft patency in a human equivalent large animal study. We hypothesized that pre-endothelialized scaECM can recruit and control infiltrating host SMCs and facilitate blood vessel regeneration while maintaining mechanical stability and avoiding graft failure through intimal hyperplasia and its associated immune response. The ability of the graft to support EC and SMC coculture was evaluated first *in vitro*. We then focused on the contribution of 2 weeks of dynamic preconditioning to reendothelialized-only graft function by culturing the lumen of scaECM grafts with the recipient autologous ECs using our custom-designed bioreactor system. Reendothelialized grafts were anastomosed as an end-to-end interposition to the porcine right common carotid artery—a rigorous test bed due to its tendency for graft blockage.[16] Finally, we studied the resulting graft patency for up to 6 weeks, monitoring signs of thrombosis and the graft's ability to control intimal hyperplasia formation through angiography at various time points and endpoint pathological evaluation.

Materials and Methods

Experimental design

Decellularized scaECM composition, structural integrity, and vascular cell support ability were characterized *in vitro* by histology and by seeding ECs and SMCs on the lumen and tunica externa, respectively, and dynamically culturing them using our custom-developed perfusion bioreactor. scaECM immunoreactivity was studied *in vitro*, and xenograft biocompatibility was demonstrated *in vivo* using a mouse subcutaneous implantation model. For immunoreactivity and biocompatibility studies, the reaction toward scaECM was compared with that elicited by commercial and FDA-approved poly-lactic-co-glycolic-acid (PLGA) and with native porcine carotid artery, as negative and positive controls, respectively. To demonstrate allogeneic functional contribution, scaECM grafts were seeded with autologous ECs and dynamically cultured before transplantation as a carotid interposition bypass graft in a pig model. Nonreendothelialized grafts and sham operation (carotid artery dissection and suture) served as the negative and positive controls, respectively. All animal experiments were carried out in accordance with the *Israeli Animal Welfare* (*Protection and Experimentation*) law and approved by the Technion Institutional Animal Care Committee. All animals received humane care in compliance with the preclinical research authority standard operating procedures. All operated vessels were monitored for up to 6 weeks by angiography and pathological assessment.

Decellularization of porcine carotid arteries

Porcine carotid arteries were harvested and decellularized as previously reported.[15,17] Briefly, arteries were washed with hypertonic and hypotonic solutions (1.1% and 0.7% NaCl) applied alternately and subjected to two 24-h cycles of enzymatic digestion (0.05% Trypsin, 0.02% EDTA) in phosphate-buffered saline (PBS; pH 7.4) at 37°C, followed by agitation in a detergent solution (1% Triton-X 100® and

1% NH_4OH in PBS) for three consecutive 72-h cycles. Samples were then washed in sterile saline, immersed in 70% ethanol for disinfection, washed in double-distilled water, and kept in sterile PBS at 4°C until utilized.

Histology

Native, decellularized, and reseeded ECM specimens and explants were gently fixed in 4% paraformaldehyde (PFA) embedded into optimal cutting temperature (OCT) cryoblocks, sectioned into 10-μm sections, and stained. Histological stains were performed as previously published for Masson's trichrome (MTC)—visualizing collagen in blue; Safranin O—visualizing glycosaminoglycans (GAG) in brown; and Verhoeff's (VER)—visualizing elastin in black.[15,17] For immunostaining, primary and secondary antibodies were used and their staining conditions are provided in Supplementary Table S1 (Supplementary Data are available online at www.liebertpub.com/tea). Bright-field color stains were imaged using Nikon Eclipse TE2000-E with a DS-Fi1 camera. All immunofluorescent stains were imaged using a Zeiss LSM700 inverted confocal microscope with a 63× oil objective with numerical aperture of 1.4.

ECM characterization

Decellularized scaECM grafts ($n=5$ grafts) were tested for their burst pressure characteristics using a custom-made setup (Supplementary Fig. S1). Briefly, grafts were subjected to rising transmural pressure by a concentric urinary balloon catheter (8Fr latex-coated catheter; BardMedical, Covington, GA) and the burst pressure was defined as the highest pressure reached before failure. Native carotid arteries ($n=5$) were tested using the same setup as control. Decellularized scaECM samples ($n=3$) were cryosectioned and stained with MTC, Safranin O, and VER stains to assess various structural components (collagen, GAG, and elastin, respectively). Quantification of GAG content was performed by the di-methyl-methylene blue method, as previously established.[18] To visualize structural integrity, scanning electron microscopy (SEM) was performed on snap-frozen and lyophilized scaECM samples as previously described[19] using an FEI-Quanta 200 SEM (OXFORD Instruments, Abington, United Kingdom; 0.6 torr, 20 KAV). Combined second harmonic generation (SHG, 810/405 nm, red) and two-photon autofluorescence (TPF, 810/520, green) imaging for collagen and elastin, respectively, were used to visualize the nonsectioned scaECM structure and major components under physiological buffer conditions, as previously reported.[20] For SHG and TPF imaging, an upright Zeiss LSM510 Meta multiphoton confocal microscope (Ti:Sapphire with laser line of 950 nm) equipped with a 25× water objective with numerical aperture of 1.0 was used. For all visualization methods, representative images are shown of at least $n=3$ randomly selected samples per group.

Ex vivo *immunogenicity evaluation*

Mouse bone marrow macrophages were isolated as previously reported,[19] seeded on six-well plates (2×10^5 cells/well), and cultured for 24 h in Dulbecco's modified Eagle medium (DMEM)-high medium with 10% fetal calf serum (FCS). Macrophages were exposed to 10 mg of minced fresh artery, minced decellularized artery, or synthetic PLGA matrices, as previously published.[21] Twenty-four hours later, nitric oxide production was evaluated using the Griess method (Promega™, Madison, WI). Macrophages were harvested and their messenger RNA (mRNA) was extracted using TriReagent and reverse transcribed in a polymerase chain reaction (PCR) cycler (PTC-200; MJ Research). The expression level of interleukin (*IL1B*) was then evaluated (normalized to *GAPDH*) by quantitative PCR (qPCR) using an Applied Biosystems 7300 system (Carlsbad, CA) with primers as detailed in Supplementary Table S2.

In vivo *evaluation of graft biocompatibility as a xenograft*

C57-J6 black mice (5–7 weeks, 20–25 g, Harlan) were randomly divided into three groups ($n=20$ mice/group): subcutaneous scaECM implantation, PLGA implantation, or sham operated to induce trauma without implant. Animals were anesthetized using a 10:1 (w/w) ketamine (Fort Dodge) and xylazine (Kepro, Deventer, Holland) cocktail (55 μg/g body weight); their back region was shaved, disinfected with 0.5% chlorhexidine gluconate in 70% alcohol, and graft specimens (5 mm long) were inserted into 1-cm-long incisions, closed, and sutured. Animals were sacrificed at designated time points post-transplantation and their inguinal lymph nodes, implants, and surrounding skin were extracted. The extracted implants were histologically stained with MTC. Lymph nodes were homogenized, their mRNA was extracted using TriReagent, and the expression of *IL1B* and tumor necrosis factor (TNF)-α levels (normalized to *GAPDH*) were quantified using qPCR with primers as depicted in Supplementary Table S2.

Primary porcine cell isolation and characterization

Porcine saphenous vein ECs (psvECs): Long segments (8 cm) of saphenous vein were aseptically extracted from anesthetized pigs, clamped, washed with PBS, and disinfected with 70% ethanol. Autologous psvECs were isolated from the lumen using 1 mg/mL collagenase-I (Worthington) in PBS for 30 min, followed by centrifugation and resuspension in M199 complete medium. Cells were seeded on six-well plates precoated with 0.2% gelatin in PBS and cultured in M199 with 20% FCS and 5 ng/mL basic fibroblast growth factor (bFGF), which was replenished daily.

Porcine carotid artery SMC (pcaSMC): Carotid artery explants were harvested in sterile conditions. Scalpel-minced 1×1-mm pieces of carotid wall were placed in 100-mm standard culture plates and grown in DMEM supplemented with 10% fetal bovine serum and antibiotics. Cells outgrew from explants within 1 week and expanded to confluence in ~4 weeks. At confluence, pcaSMC cultures had a uniform cell morphology characterized by elongated cells in parallel rows, typical of SMCs.

The isolated psvECs and pcaSMCs were examined by phase-contrast microscopy for characteristic cell morphology and their expression of lineage-positive markers was verified by flow cytometry (FACSCalibur; BD; Supplementary Table S1 and Supplementary Fig. S2).

Dynamic culture of cellularized scaECM constructs

The external layers of decellularized scaECM were seeded with pcaSMCs for 90 min, incubated in complete culture media for 24 h, and dynamically cultivated using a custom-made bioreactor as previously reported by us,[15] with slight modifications. Following a week of dynamic culture, the luminal side was seeded with psvECs. For both cell types and in both seeding instances, $0.5–1 \times 10^5$ cells/cm^2 seeding density was used. For coculture, M199 medium was supplied for the luminal feeding side and DMEM was supplied for the adventitia side; medium flow rate and pressure were adjusted to 50 mL/min and 80 mmHg, respectively. Samples were dismounted at designated time points following dynamic culture and analyzed by immunostaining (von Willebrand factor [vWF] chondroitin sulfate [CS] and smooth muscle actin [SMA]; Supplementary Table S1), WETSEM (Quantomix®), qPCR expression of remodeling-related genes (*TIMP1*, *MMP2*, and *MMP14*); and GAG quantification. Both immunostaining and WETSEM were performed after at least 20 days of dynamic cultures. For WETSEM, reendothelialized scaECM segments were stained with 1% tannic acid and 0.1% uranyl acetate (Sigma-Aldrich™), mounted on a QX-302 tissue capsule (Quantomix), and their luminal side was imaged with FEI-Quanta 200 scanning electron microscope (OXFORD Instruments). mRNA analyses were performed at 2 and 6 weeks of dynamic coculture based on primer sets defined in Supplementary Table S2. GAG quantification was performed using the dimethyl-methylene blue (DMMB) assay at designated time points of dynamic coculture, as previously described.[18]

Anastomosis of decellularized and reendothelialized biografts

Decellularized and reendothelialized ECM grafts were implanted into 6-month-old pigs ($n = 3$/group, 50–55 kg) as left carotid artery interposition biografts using a common artery exposure technique through a longitudinal incision in the mid-neck. Single-section sham operations were also performed on pigs' right carotid arteries, which were immediately sutured, and served as controls ($n = 6$ sham control vessels). Pigs were anesthetized with 100:1 (w/w) ketamine and xylazine cocktail (10.1 mg/kg body weight)

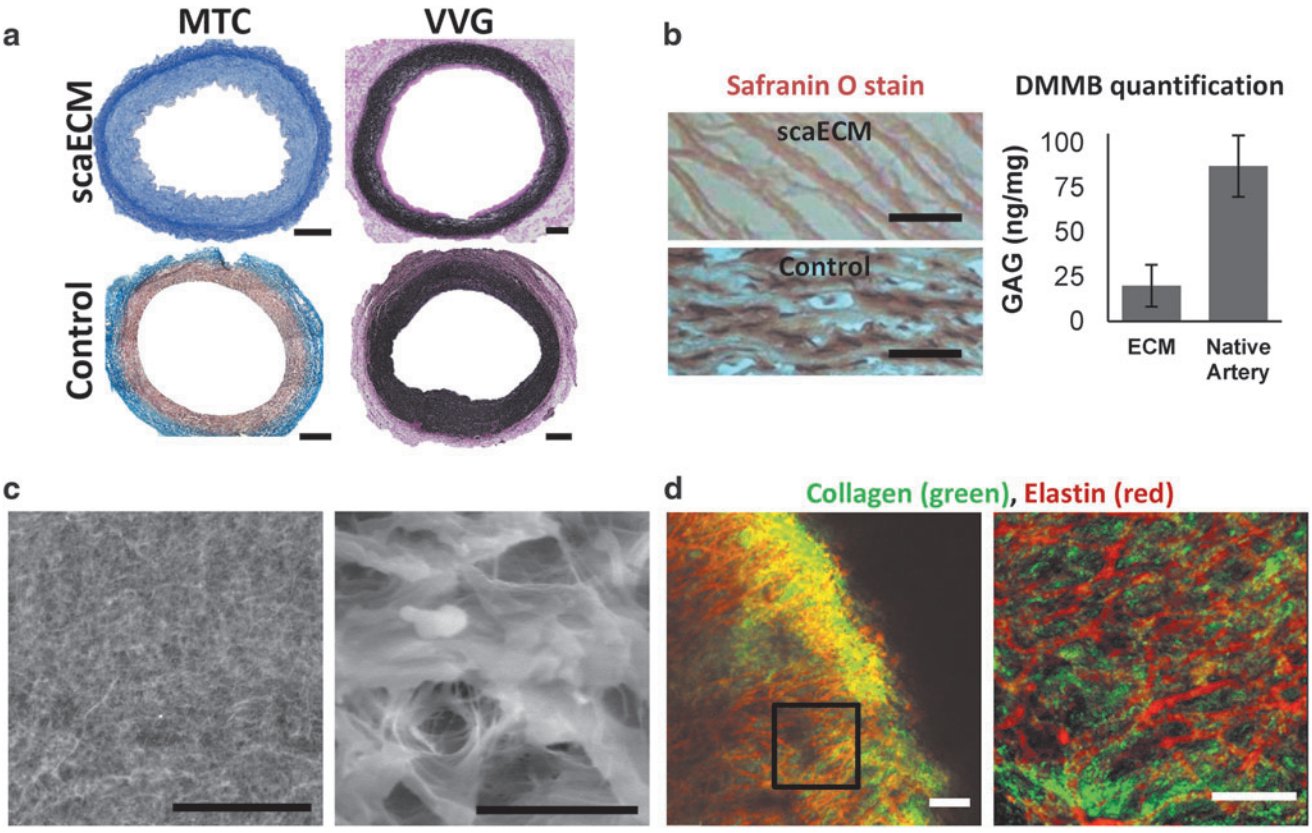

FIG. 1. Characterization of decellularized porcine scaECM. Effective decellularization and preservation of major scaECM structural components are demonstrated through histological cross-sectional stains of scaECM and a native carotid artery (positive control), as indicated **(a, b**—*left*). Collagen preservation is shown in *blue* (MTC) **(a**, *left*); elastin in *black* (Verhoeff von Gieson, VVG) **(a,** *right*); and GAG in *brown* (Safranin O) **(b,** *left*). Total GAG content was also quantified in native carotid artery and scaECM using the DMMB method **(b,** *right*). scaECM luminal ultrastructure was imaged with QuantomiX® WETSEM™ **(c)**. The interconnectivity of the major scaECM proteins was visualized through combined SHG (810/405 nm, *red*) and TPF (810/520, *green*) imaging of collagen and elastin, respectively, under physiological buffer conditions **(d)**. *Right* images represent higher magnification as indicated by scale bars **(c, d)**. Scale bars: **(a)** 500 μm; **(b**, **c**—*left*, **d)** 50 μm; **(c,** *right***)** 10 μm. DMMB, di-methyl-methylene blue; GAG, glycosaminoglycan; MTC, Masson's trichrome; scaECM, small-caliber arterial extracellular matrix; SHG, second harmonic generation; TPF, two-photon autofluorescence. Color images available online at www.liebertpub.com/tea

and 11 mg/kg body weight propofol and maintained by 2–4 L/min closed-circuit inhalation of 1.5% isoflurane (Abbott Laboratories, Abbott Park, IL) in O_2. Anesthetic depth and hemodynamic state were monitored using an invasive blood pressure (BP) transducer and electrocardiogram (ECG) sensors. Heparin (100 IU/kg body weight) was administered before arterial clamping, and the grafts (4–5 cm, one graft/pig) were inserted as an arterial bypass using end-to-end interposition with the left carotid artery and sutured with 6-0 Prolene® (Ethicon OMRIX). Grafts were then distended with heparinized saline injection to test for anastomotic sites or leakage. Arterial blood flow was reestablished and implant sites were sutured.

Graft stability and patency

Blood flow in exposed graft was measured using a Transonic T106 flow meter with a 3-mm probe positioned at the middle of the transplanted graft. Graft patency, morphology, and blood flow were evaluated by X-ray angiography under general anesthesia immediately and at 1, 2, and 6 weeks post-transplantation using a guiding catheter through the femoral artery up until 3 cm from the proximal anastomosis site. A contrast agent was administered and arteriography was performed. Patency was assessed using NIS Elements software (NIKON) by comparing graft width with that of the sham-operated arteries.

Explant characterization

Six weeks postoperation, grafts and sham-operated arteries were explanted, fixed in 10% formalin, and cut into three parts: proximal, mid, and distal. The mid parts were cut into five 5-mm-long segments for histological assessment. Blinded histological sections were evaluated by two independent Board-certified pathologists (A*Star, Singapore, Singapore; Weizmann Institute of Science, Rehovot, Israel). Thicknesses of the adventitia and media were measured using NIS Elements software and averaged from five slides per group. Fixed slides were immunostained to visualize SMC (αSMC) and EC (vWF) localization and organization, as well as innate (neutrophils, macrophages) and adaptive (B-lymphocytes) immune cells (Supplementary Table S1).

Statistical analysis

Unless otherwise stated, results are expressed as mean ± standard deviation of at least three repetitions per experimental group and time point. Statistical differences between means were determined using *t*-test for individual comparisons or by one- or two-way analysis of variance (ANOVA) when appropriate with Tukey's *post hoc* inflated α-level correction for one or more variable comparisons, respectively. Statistical significance was defined as $p < 0.05$. Representative micrographs were randomly chosen from all samples in each experiment.

Results

Decellularized scaECM characterization

Decellularized scaECM segments demonstrated retention of the major structural components of the natural arterial ECM—collagen, elastin, and at least 30% of the natural GAG content of the native artery (Fig. 1a, b). This was concomitant with preservation of burst pressure in decellularized scaECM grafts (2600 ± 400 mmHg), which was similar ($p > 0.05$, $n = 5$ samples per test group) to native tissue burst pressures (3100 ± 400 mmHg; Supplementary

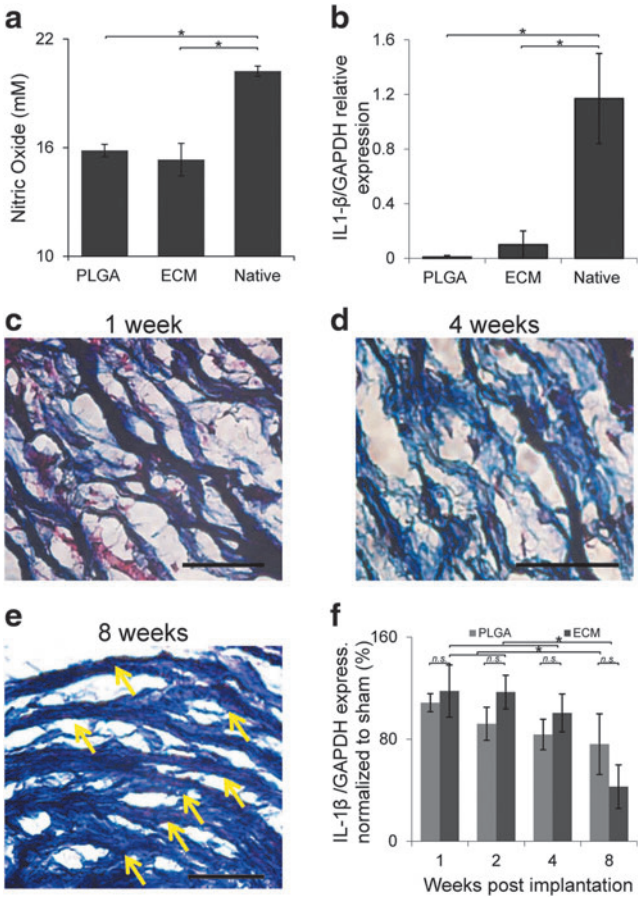

FIG. 2. Assessment of decellularized implant immunoreactivity *in vitro* and biocompatibility *in vivo*. *In vitro* immunogenicity was evaluated by exposure of scaECM, FDA-approved PLGA, and native carotid tissue (control) to isolated primary MbmMΦs and quantifying their nitric oxide secretion **(a)** and expression of *IL1B* (a proinflammatory cytokine) normalized to housekeeping *GAPDH* **(b)**. *In vivo* decellularized carotid arteries were subcutaneously implanted in C57 black mice. Representative MTC stains (*red*—cytoplasms; *black*—nuclei; *blue*—ECM fibers) of extracted implants (still largely intact) are shown at 1, 4, and 8 weeks postimplantation **(c–e)**, respectively. No signs of encapsulation were apparent (Supplementary Fig. S2) and penetrating cells were well aligned to the scaECM fiber preferred direction at 8 weeks (indicated by *yellow arrows*). Xenogeneic ECM implants do elicit a similar to PLGA (negative control) inflammatory response whose kinetic profile is demonstrated by qPCR of *IL1B*-normalized expression in draining inguinal lymph nodes through time **(f)**. *Denotes significant difference ($p < 0.05$), whereas n.s. denotes lack of statistical significance ($p > 0.05$); scale bars: 50 μm. In all assays, results represent a mean of $n = 5$ samples per group and images are representative of at least $n = 3$ images taken per sample. IL, interleukin; MbmMΦs, mouse bone marrow-derived macrophages; PLGA, poly-lactic-co-glycolic-acid; qPCR, quantitative polymerase chain reaction. Color images available online at www.liebertpub.com/tea

Fig. S1). Microscopic examination showed conservation of structural integrity, as evidenced by the dense interconnected ECM network, and the intermingled composition of collagen and elastin within the elastic lamellae of the scaECM (Fig. 1c, d). Exposure of scaECM to primary mouse bone marrow-derived macrophages (bmMΦ) elicited comparable excitation to commercially available and FDA-approved PLGA (nitric oxide secretion and expression of proinflammatory *IL1B*). In both cases, the reaction was significantly lower ($p < 0.05$) than the reaction elicited by exposure to native carotid artery serving as positive control (Fig. 2a, b). Subcutaneous xenogeneic implantation in mice revealed that the material was well tolerated by the host immune system, with no signs of encapsulation or rejection (Fig. 2 and Supplementary Fig. S3). Cell infiltration (mostly macrophages, SMCs, and fibroblasts based on pathological evaluation) subsided over time, resulting in seemingly fiber-aligned cells at 8 weeks postimplantation (Fig. 2c–e). The pathological observation was also supported by quantification of expression levels through time in the inguinal draining lymph nodes of two proinflammatory cytokines—*IL1B* (Fig. 2f) and TNF-α (Supplementary Fig. S3). This mRNA level analysis revealed a significant reduction ($p < 0.05$) in the expression level of both cytokines at 8 weeks compared with previous time points, which was similar ($p > 0.05$) to the reaction toward PLGA serving as control.

scaECM vascular cell support under physiological mimicking dynamic culture conditions

Isolated primary porcine cell sources (saphenous vein-derived ECs, psvECs, and pcaSMCs) were chosen based on their straightforward harvesting methodology. These cells displayed typical EC (homogeneous contact-inhibited monolayer) and SMC (elongated and dense fiber-like organization) morphologies, respectively, as assessed by phase-contrast microscopy; and their lineage integrity was verified through flow cytometry (Supplementary Fig. S2). Dynamic coculture of both cell types, seeded on the luminal and external surfaces of the scaECM, respectively, demonstrated vascular cell support ability of the decellularized material (Fig. 3). The psvECs self-organized on the luminal surface and formed a distinct pseudoendothelium monolayer on the internal lumen basement membrane, which did not penetrate deeper into the tissue (Fig. 3b, c). pcaSMCs, on the other hand, penetrated deeper into the scaECM wall (Fig. 3d) and expressed initial high remodeling-related genes (Fig. 3e), which were concomitant with increased secretion of GAG into the ECM matrix until a native tissue-like level was restored (Fig. 3f, g). The remodeling by SMCs seemed to be controlled given that after 6 weeks of coculture with ECs, the expression levels of all three markers significantly decreased (Fig. 3e).

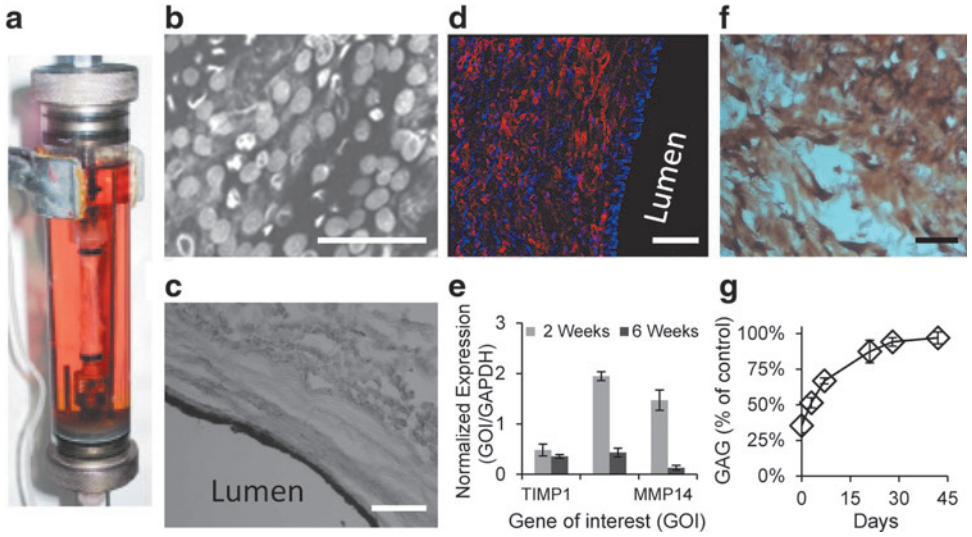

FIG. 3. Dynamic revitalization of scaECM supports compartmentalized coculture of ECs and SMCs for at least 3 weeks. *In vitro* dynamic culture system was used to mimic the physiological setting and study the ability of the scaECM graft to support endothelial and SMCs. Primary psvECs and pcaSMCs ($0.5–1 \times 10^5$ cells/cm^2) were seeded on decellularized scaECM luminal and external surfaces, respectively, and dynamically cultivated (50 mL/min and 80 mmHg) using our previously reported[15] custom-designed bioreactor, whose perfusion chamber is shown **(a)**. psvECs coated the luminal side, displayed cobblestone-like morphology as imaged with WETSEM **(b)**, and remained on the surface, forming a pseudoendothelium as verified by CD31 immunohistochemical cross-sectional stain **(c)**. In contrast, pcaSMCs penetrated deeper into the media layer, but did not penetrate the pseudoendothelium as visualized by immunofluorescent stain for αSMA (an SMC marker, Cy3, *red*) counterstained with DAPI [cell nuclei, blue **(d)** note the endothelium layer on the right-hand side is only stained with DAPI, but not with αSMA]. pcaSMC ability to remodel the dynamically cultured scaECM graft is demonstrated by qPCR quantification of the expression quantity of ECM remodeling-related genes (TIMP1, MMP2, and MMP14; normalized to GAPDH as housekeeping gene) 2 and 6 weeks postseeding, as indicated on graph **(e)**. Chondroitin sulfate (a representative GAG) secretion by the SMC is demonstrated by immunohistochemical stain **(f)**, and quantification of total GAG content through dynamic cultivation time (up to 6 weeks) is shown as percent of native porcine carotid artery tissue values (control) **(g)**. Scale bars: **(b)** 50 μm; **(c, d, f)** 100 μm. EC, endothelial cell; pcaSMC, porcine carotid artery SMC; psvECs, porcine saphenous vein ECs; SMCs, smooth muscle cells. Color images available online at www.liebertpub.com/tea

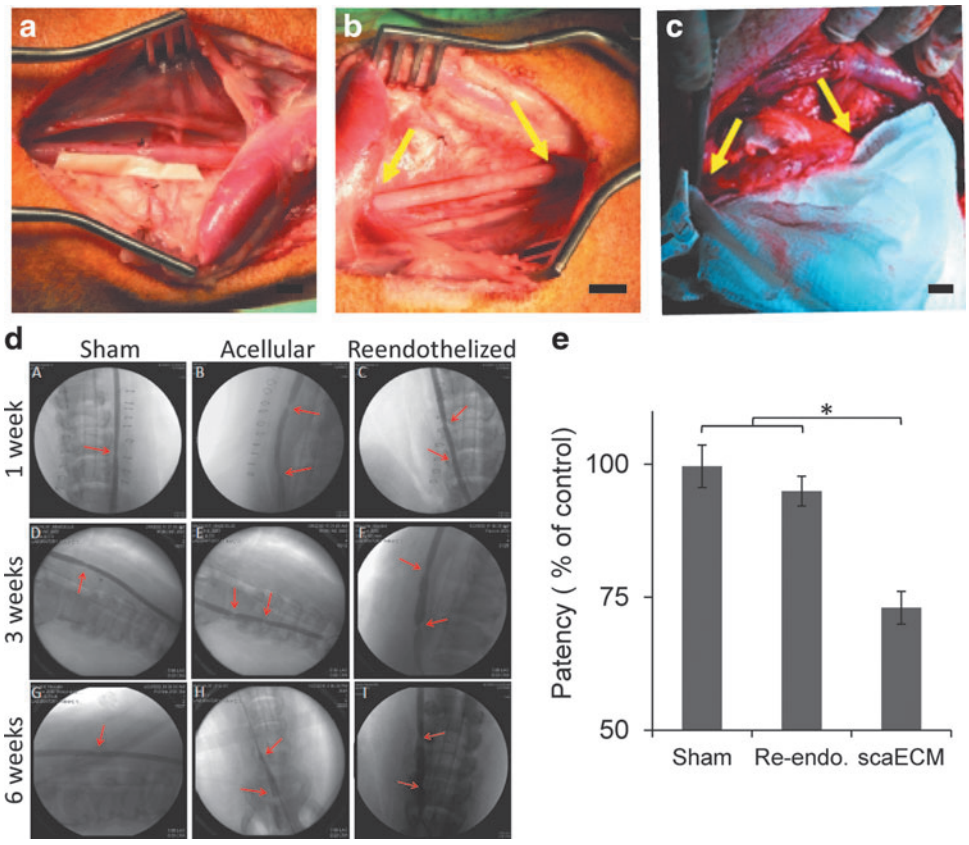

FIG. 4. scaECM transplantation as an end-to-end interposition carotid artery bypass graft. Reendothelialized allograft is positioned alongside the *left* common carotid artery **(a)**. Reendothelialized allograft was interposed to the carotid artery by end-to-end anastomosis in a swine model, 1 h **(b)** and 6 weeks **(c)** postvascular procedure. *Yellow arrows* indicate anastomotic sites. Angiograms of sham, decellularized allografts, and reendothelialized allografts 1, 3, and 6 weeks post-transplantation (as indicated in **A–I**). *Red arrows* indicate anastomotic sites **(d)**. Vascular graft patency through time is calculated from X-ray angiography images and is represented by the least square mean values as calculated from two-way ANOVA with Tukey's HSD *post hoc* correction for the effects of time and treatment groups (both significant at $p < 0.0001$) **(e)**. *Denotes significant level indicator ($p < 0.05$). Scale bars: **(a–c)** 10 mm. ANOVA, analysis of variance. Color images available online at www.liebertpub.com/tea

Biograft anastomosis to carotid artery

Graft reendothelialization—as a minimal requirement for graft patency and control of SMC recruitment, proliferation, and organization—was studied in a swine model. Dynamically reendothelialized grafts were prepared for transplantation using autologous psvECs in a process that required ~3 weeks from initial cell harvesting to allograft transplantation. One hour after anastomosis, autologous reendothelialized grafts were shown to withstand normal BP and flow (191 ± 27 mL/min), as did the sham group (197 ± 23 mL/min), with no apparent hemorrhage or rupture along the grafts or at the anastomosis sites (Fig. 4a, b). The average flow rate in the autologous reendothelialized grafts, 6 weeks after transplantation (184 ± 38 mL/min), was similar to that in the sham-operated animals (195 ± 34 mL/min, $p > 0.05$), yet significantly higher than measured on the grafts that were not pre-endothelialized (27 ± 14 mL/min, $p < 0.01$).

All animals survived the follow-up period without infections, hemorrhagic complications, graft rupture, or false aneurysms (Fig. 4c, d). Anastomosis sites of reendothelialized grafts and sham-operated controls had similar subtle arterial spasms 1 h post-transplantation, equaling 6% ± 3% reduction from the normal arterial caliber, which was significantly lower than that measured for grafts that were not reendothelialized (13% ± 6%, $p < 0.05$). Three weeks after transplantation, stenosis at the anastomosis sites of the grafts transplanted without reendothelialization increased to a level of 19% ± 4% ($p < 0.01$), while the reendothelialized grafts maintained a similar to sham group patency. Two-way ANOVA with Tukey's HSD *post hoc* correction for treatment group and time (up to 6 weeks) effect indicated that both factors significantly affected the patency rate ($p < 0.0001$). In fact, the reendothelialized graft patency profile displayed a similar to sham least square mean value and both were significantly higher than that measured for scaECM alone (Fig. 4d, e).

Graft explant pathology

Six weeks after transplantation, explanted sham anastomosis sites were slightly distorted into an oval shape, while the lumen remained fully patent (Fig. 5, top row). MTC and hematoxylin and eosin (H&E) analyses demonstrated that sham anastomosis sites had moderate multifocal granulomatous inflammation, while preserving normal vascular wall layers: intima, media (416 μm thick), and adventitia (650 μm thick), along all sides of the oval (Fig. 5, MTC and H&E as indicated). Conversely, the lumen of the nonendothelialized scaECM graft explants was filled with clotted blood, seemed narrow, and distorted with an abnormally thick media layer.

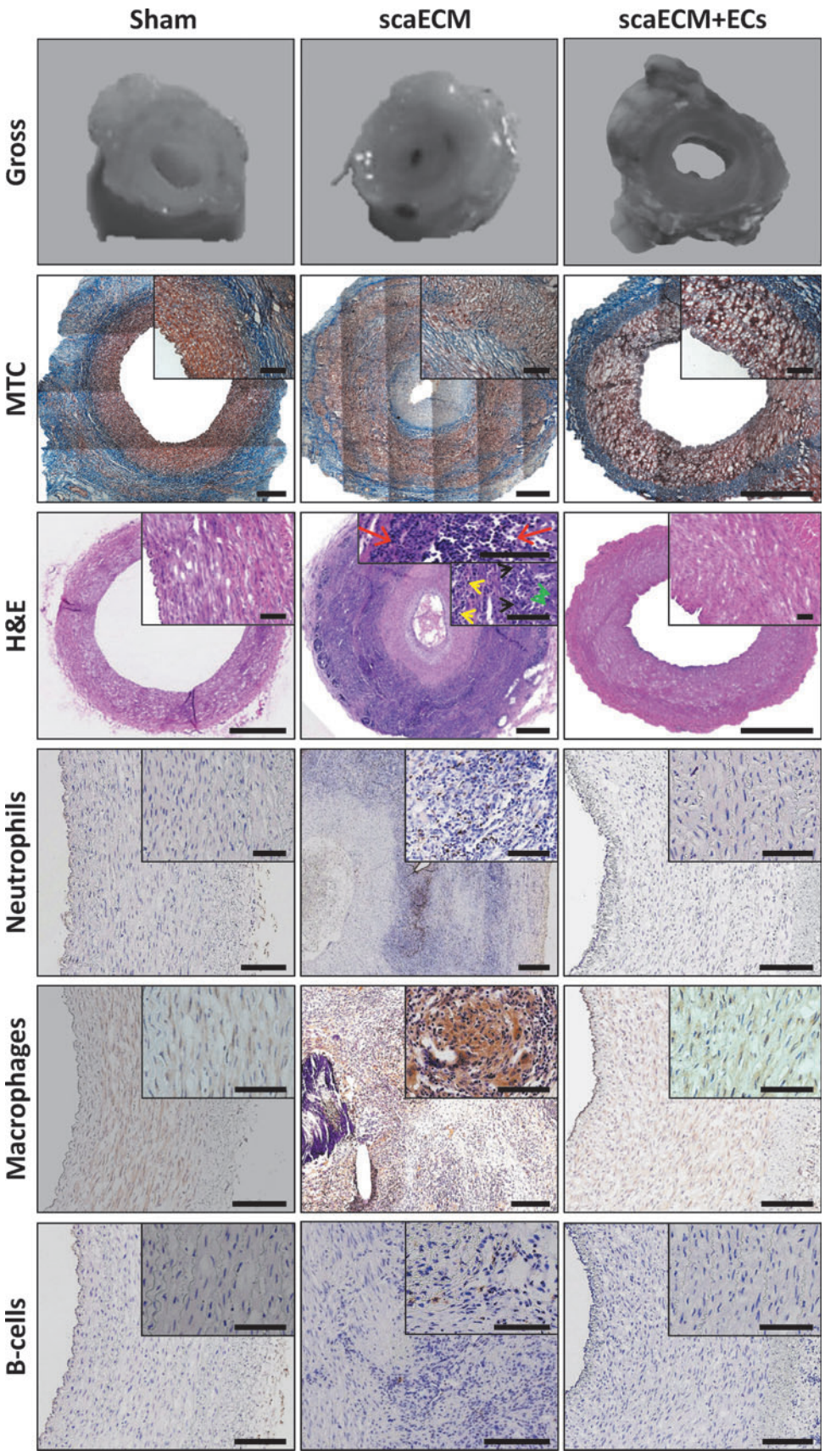

FIG. 5. Pathological evaluation of explanted scaECM and sham grafts. Gross pathological photos 6 weeks post-transplantation of recovered explants' anastomosis site and their respective MTC, H&E, and immunohistochemical stains for representative innate (neutrophils, macrophages) and adaptive (B-lymphocytes) immunity markers for sham, scaECM allografts, and autologous reendothelialized allografts (scaECM+EC), as indicated. *Insets* represent higher magnifications. *Arrowheads* in H&E images point to examples of neutrophil (*red*), macrophage (*black*), multinucleated giant cell (*green*), and lymphocyte (*yellow*) morphologies. Scale bars: overviews (MTC and H&E): 1 mm; *insets*: 100 μm; all other images: 200 μm. H&E, hematoxylin and eosin. Color images available online at www.liebertpub.com/tea

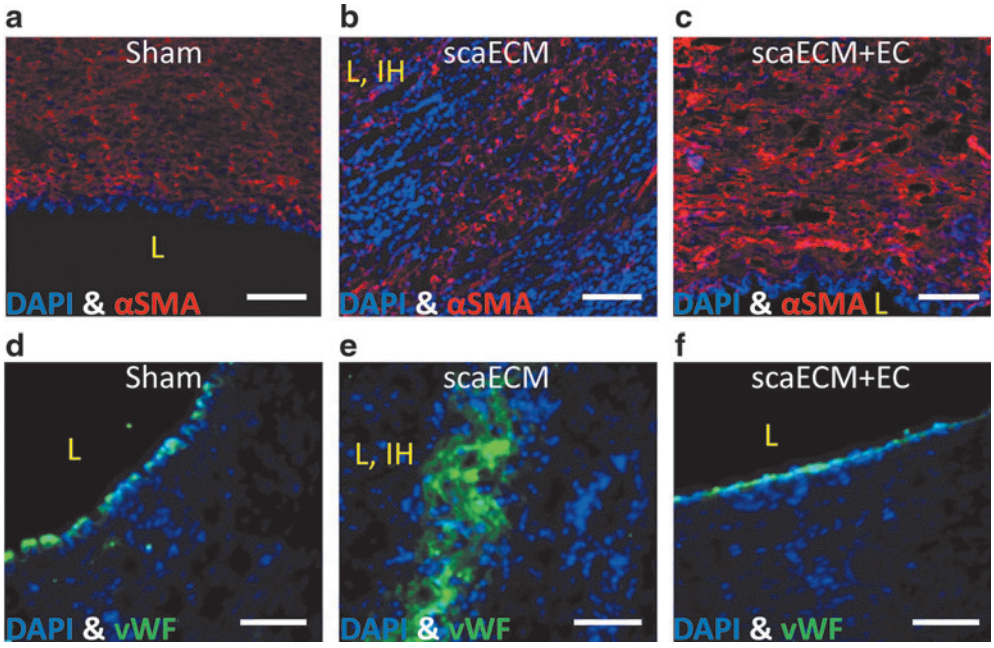

FIG. 6. Immunofluorescent visualization of ECs and SMCs in the explanted scaECM allografts—6 weeks after transplantation. Sections of sham anastomotic **(a, d)**, decellularized scaECM allograft **(b, e)**, and reendothelialized allograft (scaECM+EC) **(c, f)** stained for αSMA (Cy3—*red*, *upper panel*), vWF (FITC—*green*, *lower panel*), and counterstained with DAPI for nuclei (*blue*). Luminal area is marked by an L, intimal hyperplasia if present is marked by IH. Scale bars: **(a–f)** 100 μm. SMA, smooth muscle actin; vWF, von Willebrand factor. Color images available online at www.liebertpub.com/tea

MTC and H&E stains revealed severe neointimal hyperplasia and extensive luminal tissue ingrowths with a very small keyhole-shaped internal lumen having a cross-flow area of $<3\,mm^2$ and no apparent luminal endothelium. Instead of normal endothelium, the innermost layer of the vascular wall comprised layered extracellular eosinophilic material with irregular widths of $500 \pm 63\,\mu m$ on one side and $175 \pm 36\,\mu m$ on the contralateral side. The external layer of these grafts comprised fibrous tissue and inflammatory cells comprising both innate and adaptive immunity of mostly macrophages, neutrophils, and lymphocytes (Fig. 5, as indicated) with a concentrically arranged adventitia containing interspersed multifocal lymphohistiocytic and multinucleated giant cells and a media layer ($\sim 500\,\mu m$ wide) containing stretched and disorganized SMCs and fibroblasts. Reendothelialized grafts, similarly to sham samples, remained widely patent and slightly distorted into an oval shape with an adventitia layer, which was thicker than in the sham-operated animals. Pathological analysis revealed that the lumen was widely open and covered with an innermost endothelium layer. The thickness of the media (750 μm) and adventitia layers (550 μm) were still within the normal range despite the slight abnormality of the media morphology. Moreover, similar to the sham group, immunostaining for representative innate and adaptive immunity cells exhibited lack of neutrophils, macrophages, multinucleated giant cells, and B cells within these grafts (Fig. 5, as indicated).

Endothelial layer stability and recruitment of SMCs into the explanted grafts

Immunostaining for αSMC-actin and vWF of explants taken from anastomosis sites, 6 weeks post-transplantation, confirmed the pathological evaluation. In both sham and reendothelialized grafts, well-organized host-recruited SMCs were observed in the media layer (Fig. 6a, c, respectively) with a continuous monolayer of ECs on the lumen (Fig. 6d, f, respectively). In contrast, acellular scaECM grafts contained disorganized SMCs on both luminal and external layers of the grafts (Fig. 6b), encompassing between them several disordered and low-density layers of ECs (Fig. 6e).

Discussion

Several approaches were suggested over the past decades for functional, small-caliber (<4 mm) arterial graft (SCAG) fabrication: nondegradable synthetic vascular prosthetics; TEVG from biodegradable synthetic or natural materials (*in vitro* or *in situ*); cell sheet-based self-assembled grafts; and decellularized arterial conduits.[1,3,7] While nondegradable, clinically approved synthetic prosthetics are useful for large-caliber (>4 mm) bypassing, their clinical application for small-caliber bypassing has demonstrated dismal results.[3,7] Even when *in situ* recruited endothelialization of such grafts with modified surfaces was reported in young large animal models, recapitulating these results in clinically relevant human populations remains limited, often resulting in graft failure.[7] TEVGs from biodegradable materials and cell sheet self-assembled grafts, on the other hand, have both been specifically designed for SCAGs, with promising results.[1,3,4,22,23] In both methods, the resulting SCAG can support endothelialization and generate with time adequate mechanical properties through ECM secretion and remodeling, for instance, by SMCs. Fabrication of biomechanically stable SCAGs, however, is long and expensive as ECM secretion, remodeling, and organization processes typically require several months and mechanical stimulation *in vitro*.[3,22]

In this study, we employed an alternative approach by decellularizing readily available and inexpensive scaECMs. Others have previously pointed to the relative advantages of decellularized arterial ECMs as they inherently preserve the native artery ultrastructure and related mechanical properties (e.g., burst pressure), while avoiding the immunogenicity of donor cells.[4,24,25] In fact, several studies already showed that decellularized porcine iliac and carotid vessels may be ideal source material and that following endothelialization, these grafts remained patent for up to 130 days.[24,26] However, different ECM compositions may be expected from different decellularization procedures,[27,28] hence the product of various decellularization processes may be different between groups and care should be taken when comparing these results. For instance, too strong a decellularization process may result in excessive damage to the ECM, hampering the graft's mechanical stability, while lack of sufficient decellularization may result in triggering strong immunogenic responses and ultimately graft rejection.

We previously reported that using our decellularization protocol, some of the structural properties of the natural artery can be preserved, while increasing the stiffness of the resulting scaECM.[15] The increase in stiffness was reversible upon recellularization with SMCs; however, the underlying mechanism was not clear. As GAG washout has been previously attributed to decellularization with negative effects on mechanical properties,[28] we postulated that our decellularization protocol may lead to significant GAG washout from the matrix and that GAG quantity may be restored by repopulating SMCs. Our results clearly supported this postulation and may point to one major contribution of SMCs in decreasing the scaECM stiffness toward arterial matching values.[15] We therefore hypothesized that dynamically preendothelialized scaECM grafts can not only prevent graft failure by inhibiting blood coagulation but also recruit and control infiltrating host SMCs that increase the graft mechanical matching and stability, while limiting their uncontrolled proliferation. This control over SMC proliferation can prevent intimal hyperplasia formation and its associated inflammatory process. Seeing as intimal hyperplasia in peripheral arteries is traditionally reported at 4–6 weeks[29] from implantation, this research was specifically designed for a follow-up period of 6 weeks.

We show here that the dynamically reendothelialized scaECM grafts are mechanically stable *in vivo*, robust, and bioactive, displaying satisfactory biocompatibility, cell support, and efficacy, all while reducing production time when compared with cell sheet-based approaches. While the material itself displayed biocompatibility in both allogeneic and xenogeneic applications, the lack of such reendothelialization resulted in adverse remodeling, intimal hyperplasia formation, and associated inflammation.

One concern relating to this approach, though, is the possible triggering of a harsh immune response that may result in graft rejection due to possible incomplete decellularization and the graft xenogeneic source.[3] A recent publication by the Badylak group showed that clinically approved decellularized xenogeneic source tissues differ greatly in the extent of the host response mostly because of the prior tissue processing steps and not due to their xenogeneic nature.[30] In our study, as xenogeneic implants, our porcine decellularized scaECMs appeared to be biocompatible, with comparable immune response to that elicited by FDA-approved PLGA. The scaECM scaffold was actively remodeled by infiltrating SMCs and/or fibroblasts and overall only mildly degraded throughout the experimental timeline, indicating mechanical stability.

In conclusion, we report here that using a supportive custom-designed bioreactor system,[15] we successfully produced scaECM grafts demonstrating excellent vascular cell support ability and remodeling capability. The scaECM grafts have a uniform small diameter (3.5–4.5 mm under physiological pressure) throughout their entire length (up to 15 cm), providing a physiologically relevant source for vascular reconstructive surgeries. Furthermore, the scaECM isolation process is robust, efficient, and available as an off-the-shelf product, requiring only 3 weeks from autologous cell harvesting to implantation. In a swine SCAG bypass model, our scaECM—reendothelialized with autologous ECs—displayed excellent thromboresistance, recruited host SMCs, inhibited intimal hyperplasia and its associated inflammation, and remained patent throughout the entire follow-up period (up to 6 weeks). We therefore suggest that with good laboratory practice and under careful quality control of source materials, this strategy may offer a viable option for SCAGs with a view for wide clinical applicability.

Acknowledgments

This work was supported by an NOFAR grant (Israeli chief scientist program). The authors would like to acknowledge the experimental animal facility at the Rappaport Medical School and the Microscopy Unit of the Life Sciences and Engineering Infrastructure Center (Technion, Haifa, Israel) for their expert technical assistance during completion of the present article.

Disclosure Statement

No competing financial interests exist.

References

1. Natasha, G., Tan, A., Gundogan, B., Farhatnia, Y., Nayyer, L., Mahdibeiraghdar, S., Rajadas, J., De Coppi, P., Davies, A.H., and Seifalian, A.M. Tissue engineering vascular grafts a fortiori: looking back and going forward. Expert Opin Biol Ther **15,** 231, 2015.
2. Peck, M., Dusserre, N., McAllister, T.N., and L'Heureux, N. Tissue engineering by self-assembly. Materials Today **14,** 218, 2011.
3. Huang, A.H., and Niklason, L.E. Engineering of arteries in vitro. Cell Mol Life Sci **71,** 2103, 2014.
4. Pashneh-Tala, S., MacNeil, S., and Claeyssens, F. The tissue-engineered vascular graft—past, present, and future. Tissue Eng Part B Rev **22,** 68, 2015.
5. Li, S., Sengupta, D., and Chien, S. Vascular tissue engineering: from in vitro to in situ. Wiley Interdiscip Rev Syst Biol Med **6,** 61, 2014.
6. Beattie, A.J., Gilbert, T.W., Guyot, J.P., Yates, A.J., and Badylak, S.F. Chemoattraction of progenitor cells by remodeling extracellular matrix scaffolds. Tissue Eng Part A **15,** 1119, 2009.
7. Zilla, P., Bezuidenhout, D., and Human, P. Prosthetic vascular grafts: wrong models, wrong questions and no healing. Biomaterials **28,** 5009, 2007.

8. Ku, D.N., and Allen, R.C. Vascular Grafts in: The Biomedical Engineering Handbook. 2nd ed. Boca Raton, FL: CRC Press LLC, 2000.
9. Naito, Y., Shinoka, T., Duncan, D., Hibino, N., Solomon, D., Cleary, M., Rathore, A., Fein, C., Church, S., and Breuer, C. Vascular tissue engineering: towards the next generation vascular grafts. Adv Drug Deliv Rev **63,** 312, 2011.
10. Furchgott, R.F., and Zawadzki, J.V. The obligatory role of endothelial cells in the relaxation of arterial smooth muscle by acetylcholine. Nature **288,** 373, 1980.
11. Autio, I., Malo-Ranta, U., Kallioniemi, O.P., and Nikkari, T. Cultured bovine aortic endothelial cells secrete factor(s) chemotactic for aortic smooth muscle cells. Artery **16,** 72, 1989.
12. Cybulsky, M.I., and Gimbrone, M.A., Jr. Endothelial expression of a mononuclear leukocyte adhesion molecule during atherogenesis. Science **251,** 788, 1991.
13. Casscells, W. Migration of smooth muscle and endothelial cells. Critical events in restenosis. Circulation **86,** 723, 1992.
14. Lavin, B., Gomez, M., Pello, O.M., Castejon, B., Piedras, M.J., Saura, M., and Zaragoza, C. Nitric oxide prevents aortic neointimal hyperplasia by controlling macrophage polarization. Arterioscler Thromb Vasc Biol **34,** 1739, 2014.
15. Dahan, N., Zarbiv, G., Sarig, U., Karram, T., Hoffman, A., and Machluf, M. Porcine small diameter arterial extracellular matrix supports endothelium formation and media remodeling forming a promising vascular engineered biograft. Tissue Eng Part A **18,** 411, 2012.
16. Quint, C., Kondo, Y., Manson, R.J., Lawson, J.H., Dardik, A., and Niklason, L.E. Decellularized tissue-engineered blood vessel as an arterial conduit. Proc Natl Acad Sci U S A **108,** 9214, 2011.
17. Eitan, Y., Sarig, U., Dahan, N., and Machluf, M. Acellular cardiac extracellular matrix as a scaffold for tissue engineering: In-vitro cell support, remodeling and biocompatibility. Tissue Eng Part C Methods **16,** 671, 2010.
18. Coulson-Thomas, V.J., and Gesteira, T.F. Dimethylmethylene blue assay (DMMB). Bioprotocol **4,** 1, 2014.
19. Sarig, U., Gigi, A.Y., Yao, W., Bronshtein, T., Dahan, N., Freddy, B.Y., Venkatraman, S.S., and Machluf, M. Thick acellular heart extracellular matrix with inherent vasculature: a potential platform for myocardial tissue regeneration. Tissue Eng Part A **18,** 2125, 2012.
20. Zoumi, A., Lu, X., Kassab, G.S., and Tromberg, B.J. Imaging coronary artery microstructure using second-harmonic and two-photon fluorescence microscopy. Biophys J **87,** 2778, 2004.
21. Lesman, A., Koffler, J., Atlas, R., Blinder, Y.J., Kam, Z., and Levenberg, S. Engineering vessel-like networks within multicellular fibrin-based constructs. Biomaterials **32,** 7856, 2011.
22. Peck, M., Gebhart, D., Dusserre, N., McAllister, T.N., and L'Heureux, N. The evolution of vascular tissue engineering and current state of the art. Cells Tissues Organs **195,** 144, 2012.
23. Tondreau, M.Y., Laterreur, V., Gauvin, R., Vallieres, K., Bourget, J.M., Lacroix, D., Tremblay, C., Germain, L., Ruel, J., and Auger, F.A. Mechanical properties of endothelialized fibroblast-derived vascular scaffolds stimulated in a bioreactor. Acta Biomater **18,** 176, 2015.
24. Kaushal, S., Amiel, G.E., Guleserian, K.J., Shapira, O.M., Perry, T., Sutherland, F.W., Rabkin, E., Moran, A.M., Schoen, F.J., Atala, A., Soker, S., Bischoff, J., and Mayer, J.E., Jr. Functional small-diameter neovessels created using endothelial progenitor cells expanded ex vivo. Nat Med **7,** 1035, 2001.
25. Mahara, A., Somekawa, S., Kobayashi, N., Hirano, Y., Kimura, Y., Fujisato, T., and Yamaoka, T. Tissue-engineered acellular small diameter long-bypass grafts with neointima-inducing activity. Biomaterials **58,** 54, 2015.
26. Tillman, B.W., Yazdani, S.K., Neff, L.P., Corriere, M.A., Christ, G.J., Soker, S., Atala, A., Geary, R.L., and Yoo, J.J. Bioengineered vascular access maintains structural integrity in response to arteriovenous flow and repeated needle puncture. J Vasc Surg **56,** 783, 2012.
27. Badylak, S.F., Taylor, D., and Uygun, K. Whole-organ tissue engineering: Decellularization and recellularization of three-dimensional matrix scaffolds. Annu Rev Biomed Eng **13,** 27, 2011.
28. Crapo, P.M., Gilbert, T.W., and Badylak, S.F. An overview of tissue and whole organ decellularization processes. Biomaterials **32,** 3233, 2011.
29. Houbballah, R., Robaldo, A., Albadawi, H., Titus, J., and LaMuraglia, G.M. A novel model of accelerated intimal hyperplasia in the pig iliac artery. Int J Exp Pathol **92,** 422, 2011.
30. Badylak, S.F. Decellularized allogeneic and xenogeneic tissue as a bioscaffold for regenerative medicine: factors that influence the host response. Ann Biomed Eng **42,** 1517, 2014.

Address correspondence to:
Marcelle Machluf, PhD
Faculty of Biotechnology and Food Engineering
Technion–Israel Institute of Technology
Haifa 32000
Israel

E-mail: machlufm@tx.technion.ac.il

Received: April 3, 2016
Accepted: October 6, 2016
Online Publication Date: December 20, 2016